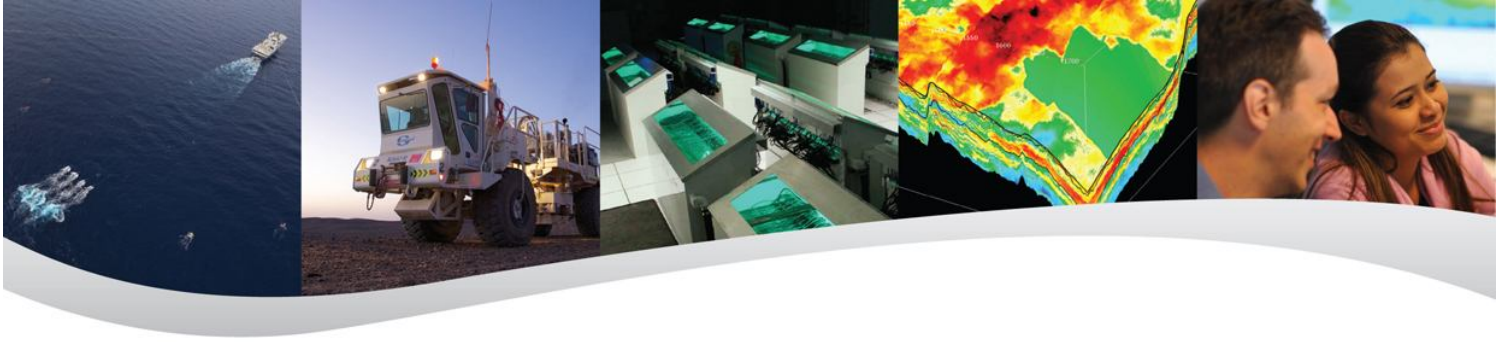


Kirkland Lake Gold
FALCON® Airborne Gravity Gradiometer Survey
Fosterville, Victoria

Project Number: 803064

Logistics and Processing Report

CGG Aviation (Australia) Pty Ltd
Level 1, 1 Ord Street
West Perth, Western Australia, 6005
AUSTRALIA
Tel: +61 (8) 9214-6200, Fax: +61 (8) 9214-6222

Passion for Geoscience
cgg.com

Table of contents

1 INTRODUCTION 5
1.1 Survey Location 5
1.2 General Disclaimer 6
2 SUMMARY OF SURVEY PARAMETERS 7
2.1 Survey Area Specifications 7
2.2 Data Recording 8
2.3 Project Safety Plan, HSE Summary 9
3 FIELD OPERATIONS 10
3.1 Operations 10
3.2 Base Stations 10
3.2.1 GPS Base Station 10
3.2.2 Magnetometer Base Station (CF1) 10
3.3 Field Personnel 10
4 QUALITY CONTROL RESULTS 11
4.1 Survey acquisition issues 11
4.2 Flight Path Map 12
4.3 Turbulence 13
4.4 AGG System Noise 14
4.5 Digital Terrain Model 17
4.6 Terrain Clearance 19
5 FALCON® AIRBORNE GRAVITY GRADIENT (AGG) RESULTS 20
5.1 Processing Summary 20
5.2 FALCON® Airborne Gravity Gradiometer Data 20
5.3 Radar Altimeter Data 21
5.4 Laser Scanner Data 21
5.5 Positional Data 21
5.6 Terrain Correction 21
5.7 Mean-Removal Levelling 21
5.8 Micro-levelling 21
5.9 Enhanced Processing 21
5.10 FALCON® Airborne Gravity Gradient Data - G_{DD} & g_D 22
5.11 Conforming gD to regional gravity 25
6 MAGNETIC RESULTS 27
6.1 Processing Summary 27
6.2 Aeromagnetic Data 27
6.3 Radar Altimeter Data 27
6.4 Positional Data 28
6.5 Lag Correction 28
6.6 IGRF Correction 28
6.7 Diurnal Subtraction 28
6.8 Height Correction 28

6.9 Micro-levelling 28
6.10 Total Magnetic Intensity 28
7 APPENDIX I - SURVEY EQUIPMENT 30
7.1 Survey Aircraft 30
7.2 FALCON® Airborne Gravity Gradiometer 30
7.3 Airborne Data Acquisition Systems 30
7.4 Aerial and Ground Magnetometers 30
7.5 Real-Time Differential GPS 30
7.6 GPS Base Station Receiver 30
7.7 Altimeters 31
7.8 Laser Scanner 31
7.9 Data Processing Hardware and Software 31
8 APPENDIX II - SYSTEM TESTS 32
8.1 Instrumentation Lag 32
8.2 Radar Altimeter Calibration 32
8.3 Magnetometer Compensation 32
8.4 FALCON® AGG Noise Measurement 32
8.5 Daily Calibrations 32
8.5.1 Magnetic Base Station Time Check 32
8.5.2 FALCON® AGG Calibration 32
9 APPENDIX III - FALCON® AGG DATA & PROCESSING 33
9.1 Nomenclature 33
9.2 Units 33
9.3 FALCON® Airborne Gravity Gradiometer Surveys 33
9.4 Gravity Data Processing 33
9.5 Aircraft Dynamic Corrections 34
9.6 Self-gradient Corrections 34
9.7 Laser Scanner Processing 34
9.8 Terrain Corrections 34
9.9 Tie line Levelling 34
9.10 Transformation into GDD & g_D 35
9.11 Terrain Corrections Using Alternate Terrain Densities 35
9.12 Noise & Signal 36
9.13 Risk Criteria in Interpretation 36
9.14 References 36
10 APPENDIX IV - FINAL PRODUCTS 38

Figures

Figure 1: Fosterville – Survey Area Location 5
Figure 2: Fosterville – Flight Path map 12
Figure 3: Fosterville – Turbulence (millig where g = 9.80665 m/sec/sec) 13
Figure 4: Fosterville – System Noise NE (eotvos) 15
Figure 5: Fosterville – System Noise UV (eotvos) 16
Figure 6: Fosterville – Final Digital Terrain Model (metres, referenced to the EGM96 geoid) 18
Figure 7: Fosterville – Terrain clearance derived from laser scanner data (metres) 19
Figure 8: FALCON® AGG Data Processing 20
Figure 9: Fosterville – Vertical Gravity Gradient (GDD) from equivalent source processing (eotvos) 23
Figure 10: Fosterville – Vertical Gravity (gD) from equivalent source processing (mGal) 24
Figure 11: Fosterville – Vertical Gravity (gD) from equivalent source processing conformed to regional gravity data (milligal). 26
Figure 12: Magnetic Data Processing 27
Figure 13: Fosterville – Total Magnetic Intensity (nT) 29

Tables

Table 1: Fosterville Specifications 7
Table 2: Fosterville – Survey Boundary Coordinates 8
Table 3: Field Personnel 10
Table 4: Final FALCON® AGG Digital Data – Geosoft Database Format 40
Table 5: Final Aeromagnetic Digital Data – Geosoft Database Format 41
Table 6: Final magnetic and AGG Grids – ERMapper Format 42

1 INTRODUCTION

CGG conducted a high-sensitivity magnetic and **FALCON**® Airborne Gravity Gradiometer (AGG) survey over the Fosterville survey area under contract with Kirkland Lake Gold.

1.1 Survey Location

The Fosterville survey area is centred on longitude 144° 26' E, latitude 36º 30' S (see the location map in *Figure 1*).

The production flights took place during February 2019 with the first production flight taking place on February 18th and the final flight taking place on February 25th. To complete the survey area coverage a total of 13 production flights were flown, for a combined total of 5537 line kilometres of data acquired.

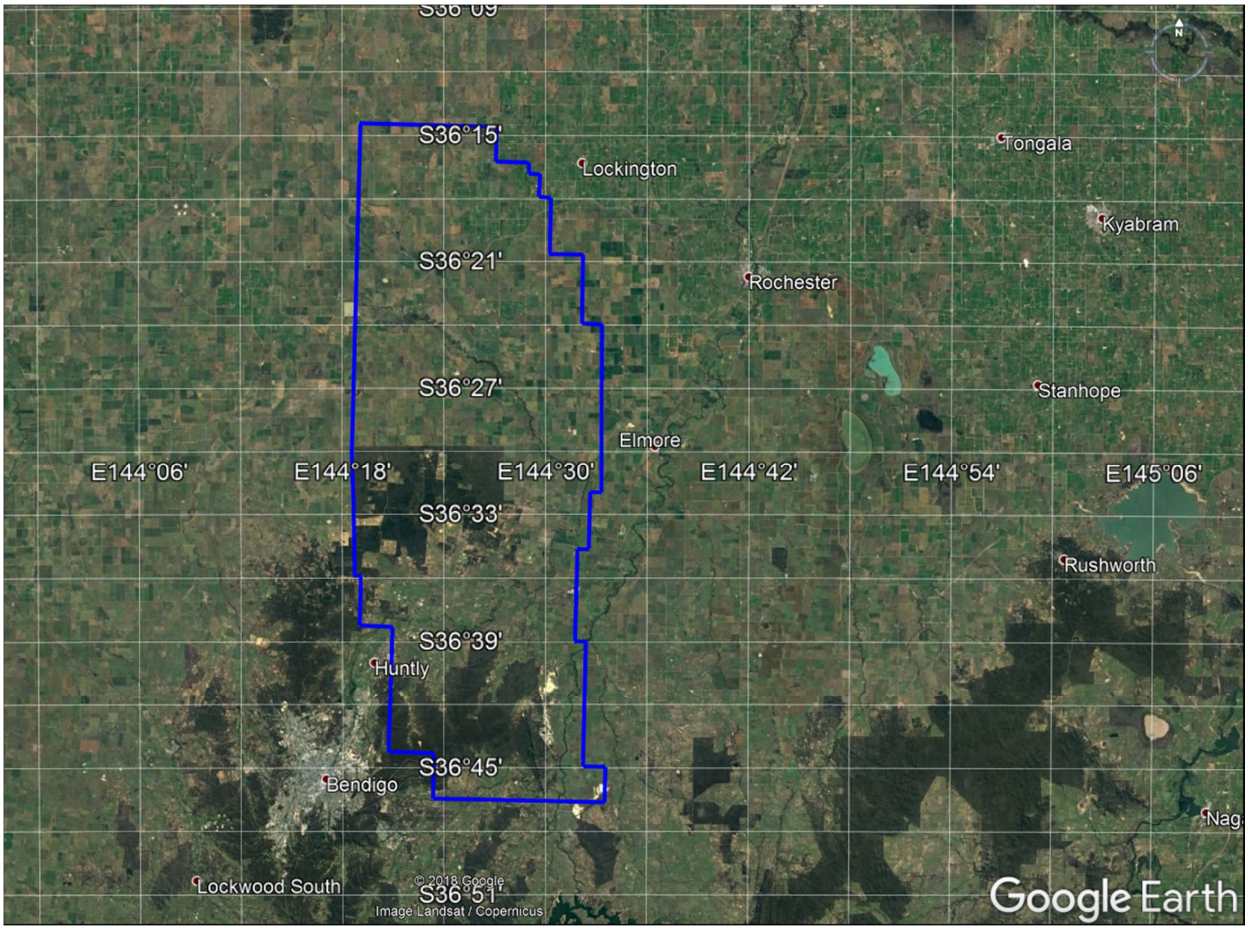


Figure 1: Fosterville – Survey Area Location

1.2 General Disclaimer

It is CGG's understanding that the data and report provided to the client are to be used for the purpose agreed between the parties. That purpose was a significant factor in determining the scope and level of the Services being offered to the Client. Should the purpose for which the data and report are used change, the data and report may no longer be valid or appropriate and any further use of, or reliance upon, the data and report in those circumstances by the Client without CGG's review and advice shall be at the Client's own and sole risk.

The Services were performed by CGG exclusively for the purposes of the Client. Should the data and report be made available in whole or part to any third party, and such party relies thereon, that party does so wholly at its own and sole risk and CGG disclaims any liability to such party.

Where the Services have involved CGG's use of any information provided by the Client or third parties, upon which CGG was reasonably entitled to rely, then the Services are limited by the accuracy of such information. CGG is not liable for any inaccuracies (including any incompleteness) in the said information, save as otherwise provided in the terms of the contract between the Client and CGG.

2 SUMMARY OF SURVEY PARAMETERS

2.1 Survey Area Specifications

Total Kilometres (km)	5537
Clearance Method	Drape
Minimum Drape Height (m	80
Traverse Line Direction (deg.)	90 / 270
Traverse Line Spacing (m)	200

Table 1: Fosterville Specifications

The survey block is defined by the coordinates in *Table 2*, in UTM Zone 55S projection, referenced to the WGS84 datum.

Corner Number	Easting	Northing
1	259014	5986020
2	271038	5986020
3	271038	5982989
4	273936	5982989
5	274003	5982023
6	274969	5981989
7	274902	5980024
8	275968	5979958
9	276001	5974961
10	278932	5974995
11	278999	5968966
12	280764	5968933
13	280997	5959007
14	281114	5954194
15	280115	5954177
16	280115	5949215
17	279132	5949181
18	279116	5941154
19	280081	5941187
20	280115	5930179
21	282097	5930196
22	282097	5927098
23	266992	5927015
24	266958	5930979
25	262961	5931012
26	263028	5941970
27	260130	5942037
28	260130	5946333
29	259577	5946331
30	259297	5952622
31	259027	5957205

Table 2: Fosterville – Survey Boundary Coordinates

2.2 Data Recording

The following parameters were recorded during the course of the survey:

- **FALCON® AGG data:** recorded at different intervals.
- **Airborne total magnetic field:** recorded with a 0.1 s sampling rate.
- **Terrain clearance:** provided by the radar altimeter at intervals of 0.1 s.
- **Airborne GPS positional data** (latitude, longitude, height, time and raw range from each satellite being tracked): recorded at intervals of 1 s.
- **Time markers:** in digital data.
- **Ground total magnetic field:** recorded with a 1 s sampling rate.
- **Ground based GPS positional data** (latitude, longitude, height, time and raw range from each satellite being tracked): recorded at intervals of 1 s.
- **Ground surface below aircraft:** mapped by the laser scanner system, scanning at 36 times per second, recording 276 returns per scan (when within range of the instrument and in the absence of thick vegetation).

2.3 Project Safety Plan, HSE Summary

A Job Safety Plan and Job Safety Analysis was prepared and implemented in accordance with the CGG Occupational Safety and Health Management System.

3 FIELD OPERATIONS

3.1 Operations

The survey was based out of Bendigo, Victoria. The survey aircraft was operated from Bendigo Airport using aviation fuel available on site. A temporary office was set up in Bendigo where all survey operations were run and the post-flight data verification was performed.

3.2 Base Stations

A dual frequency GPS base station was set up at the airport in order to correct the raw GPS data collected in the aircraft. A secondary GPS base station was available but was not required.

3.2.1 GPS Base Station

Location: Bendigo Airport

Date: February 24th, 2019

Latitude: 36º 44' 20.46516 " S

Longitude: 144º 19' 29.41349" E

Height: 217.033 m ellipsoidal

3.2.2 Magnetometer Base Station (CF1)

Location: Bendigo Airport

Date: February 24th, 2019

Latitude: 36º 44' 20.45 " S

Longitude: 144º 19' 29.48" E

Base: 59380 nT

3.3 Field Personnel

The following technical personnel participated in field operations:

Crew Leader:	J. Wessels
Pilots:	D. Phillips, G. Henry and R. Spinks, O. Nelson
Technician:	D. Little
Engineer:	M. Drury
Project Manager:	J. Wessels
Final QC and Processing:	A. Carbone

Table 3: Field Personnel

4 QUALITY CONTROL RESULTS

4.1 Survey acquisition issues

During the course of the survey there were no data quality issues with:

- AGG instrumentation
- Magnetic and GPS base stations
- Airborne magnetometer system
- Data acquisition systems
- Radar altimeter
- Laser scanner

4.2 Flight Path Map

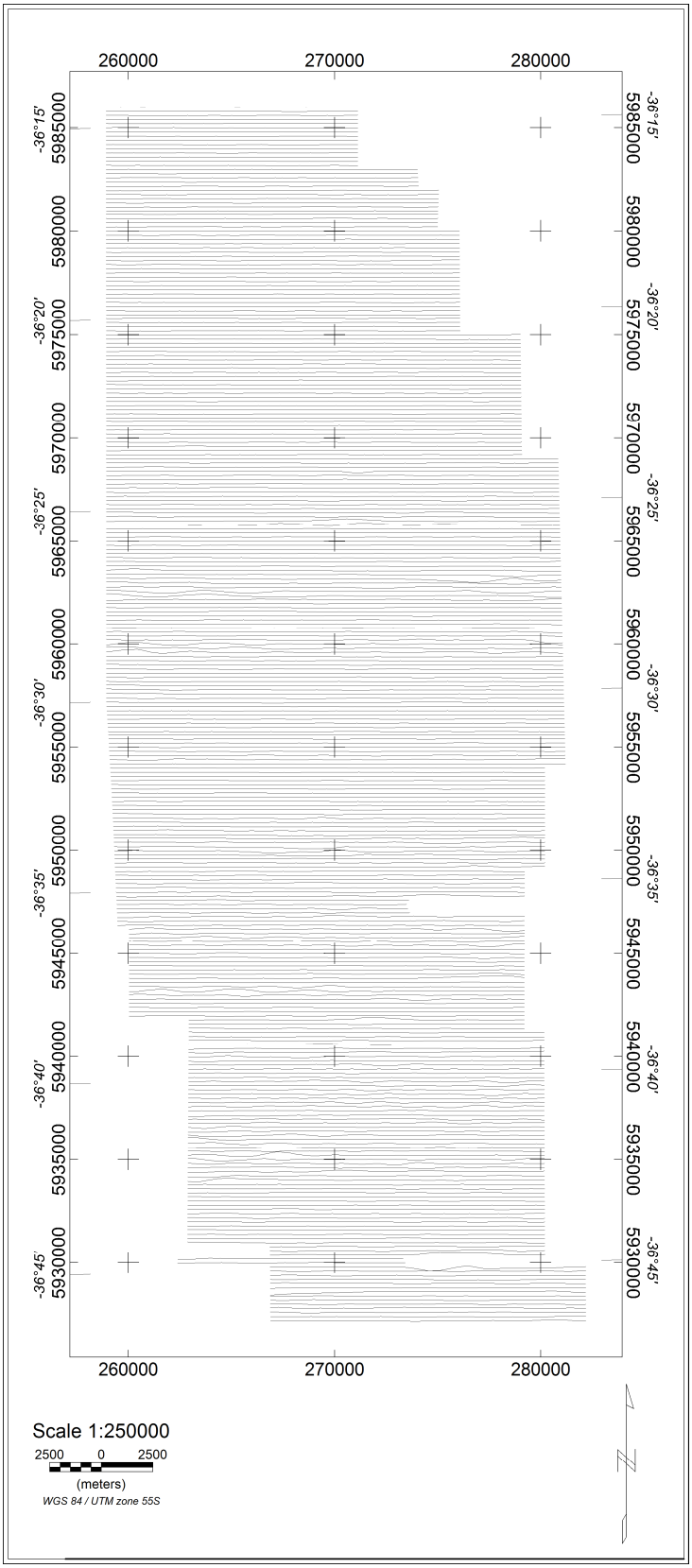


Figure 2: Fosterville – Flight Path map

4.3 Turbulence

The mean turbulence recorded in the Fosterville survey area was 81.5 milli g (where g = 9.80665 m/sec/sec). Turbulence was variable, but was high on most survey days. The typical pattern for a given flight was for turbulence to commence at a low level and then increase throughout the flight. The turbulence pattern across the survey area is shown in *Figure 3*.

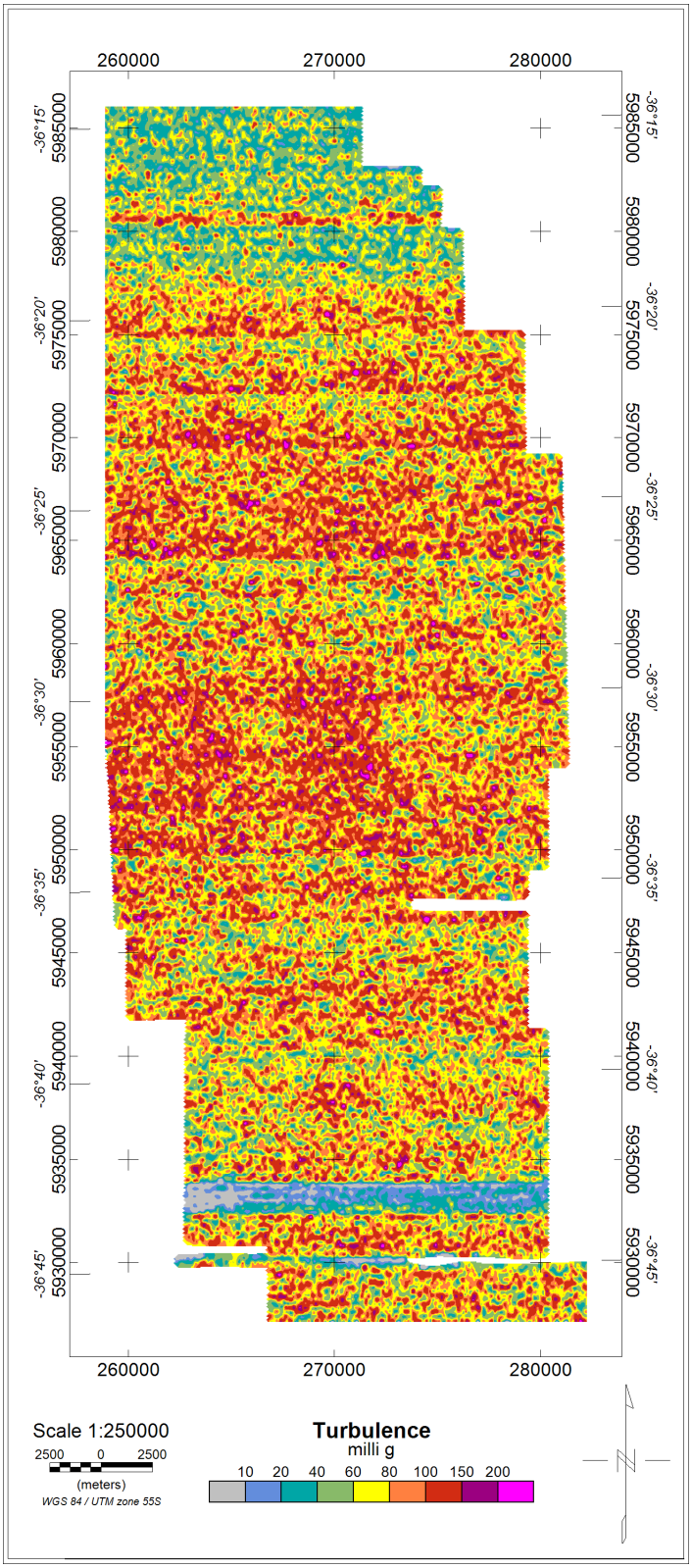


Figure 3: Fosterville – Turbulence (millig where g = 9.80665 m/sec/sec)

4.4 AGG System Noise

The system noise is defined to be the standard deviation of half the difference between the A & B complements, for each of the NE and UV curvature components. The results for this survey were very good with values of 2.87 E and 2.75 E for NE and UV respectively.

Figure 4 and *Figure 5* provide a representation of the variation in this standard deviation for each component. This is achieved by gridding a rolling measurement of standard deviation along each line using a window length of 100 data points.

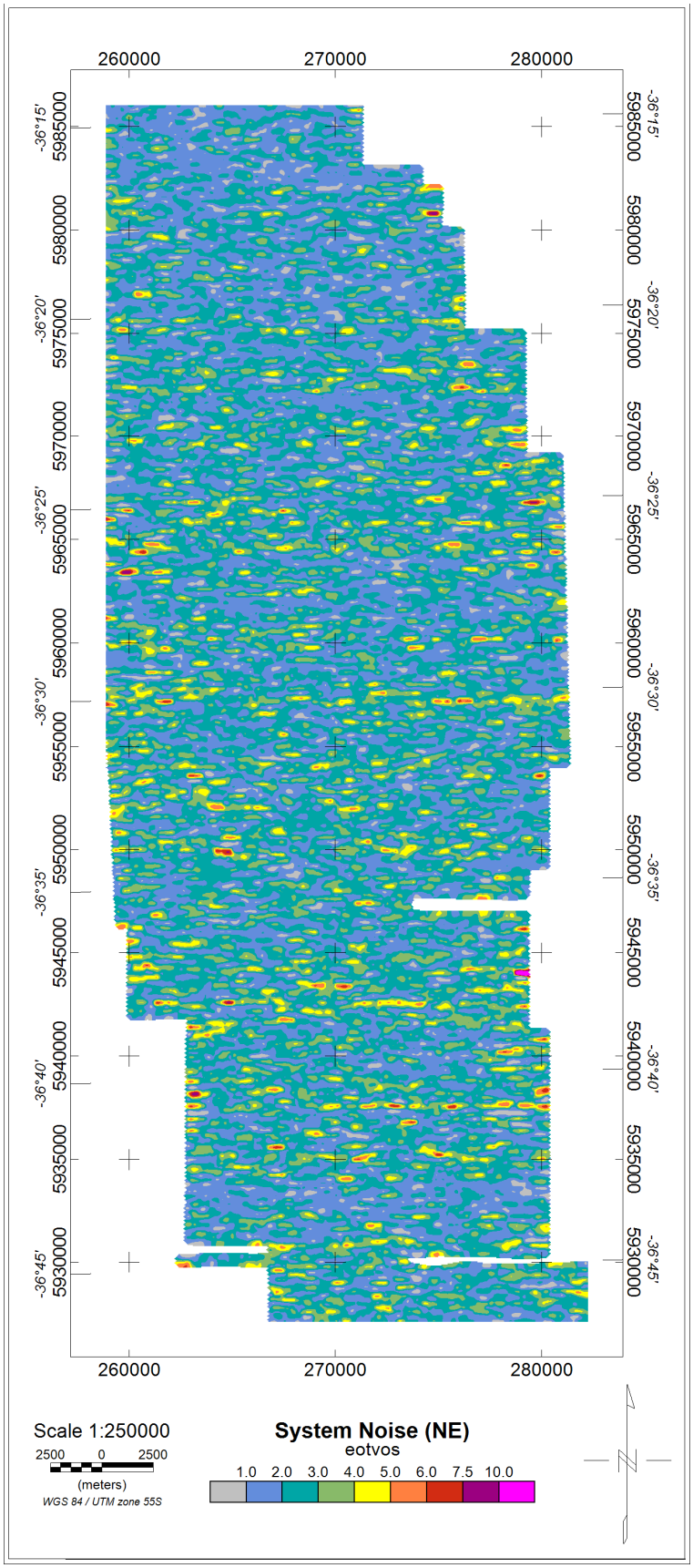


Figure 4: Fosterville – System Noise NE (eotvos)

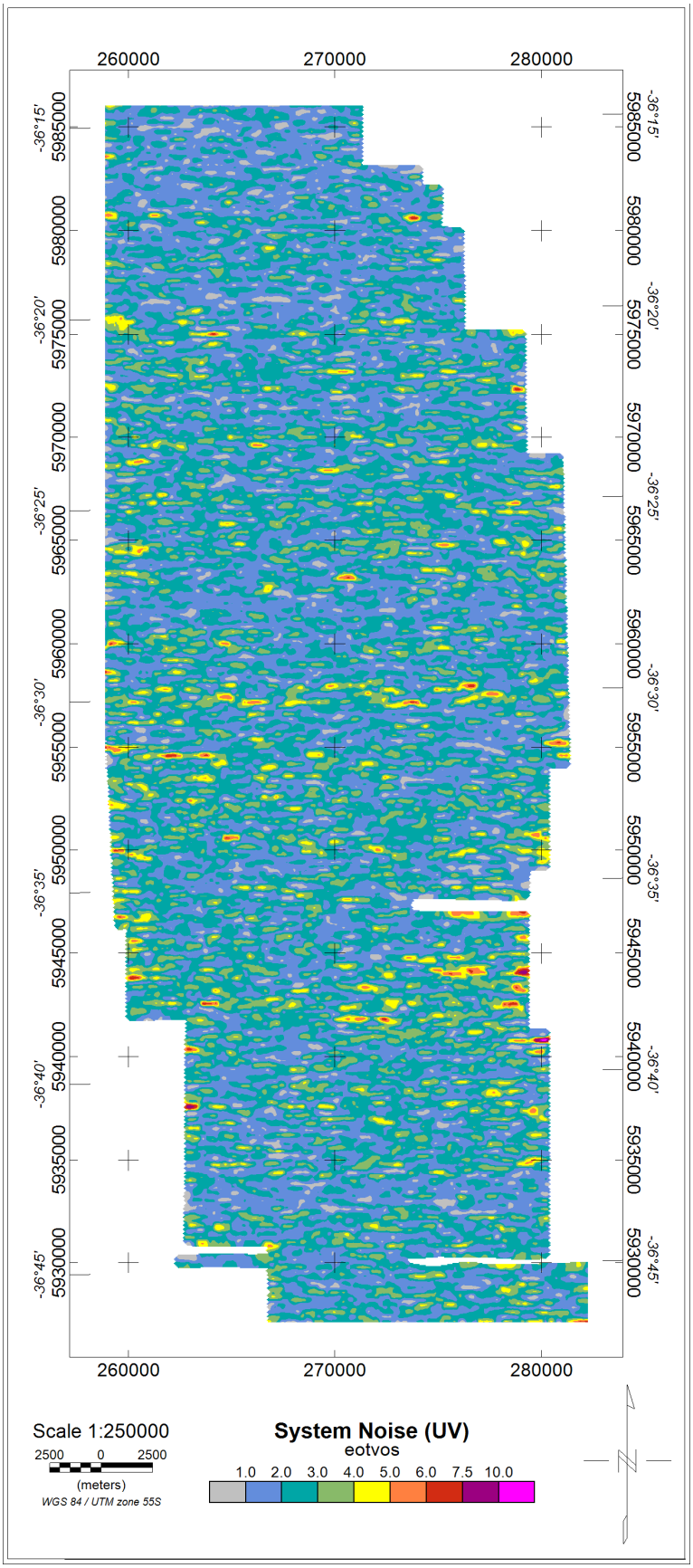


Figure 5: Fosterville – System Noise UV (eotvos)

4.5 Digital Terrain Model

Laser scanner range data were combined with GPS position and height data. An undulation correction was applied to the GPS data prior to scanner processing to adjust the height above the WGS84 ellipsoid to height above the geoid by applying the Earth Gravitational Model 1996 (EGM96)) using Novatel's Waypoint Grafnav GPS processing software . The output of combining the scanner range data with the GPS is a "swath" of terrain elevations extending either side of the aircraft flight path. Width and sample density of this swath varies with aircraft height. Typical values are 100 to 150 metres and 5 to 10 metres respectively.

Because terrain correction of AGG data requires knowledge of the terrain at distances up to at least 10 km from the data location, laser scanner data collected only along the survey line path must be supplemented by data from another source. For this purpose, Geoscience Australia 1 second SRTM (DEM-S) data are used. This smoothed DEM has reduced noise when compared to SRTM in low relief areas.

Figure 6 shows the final Digital Terrain Model for the survey area.

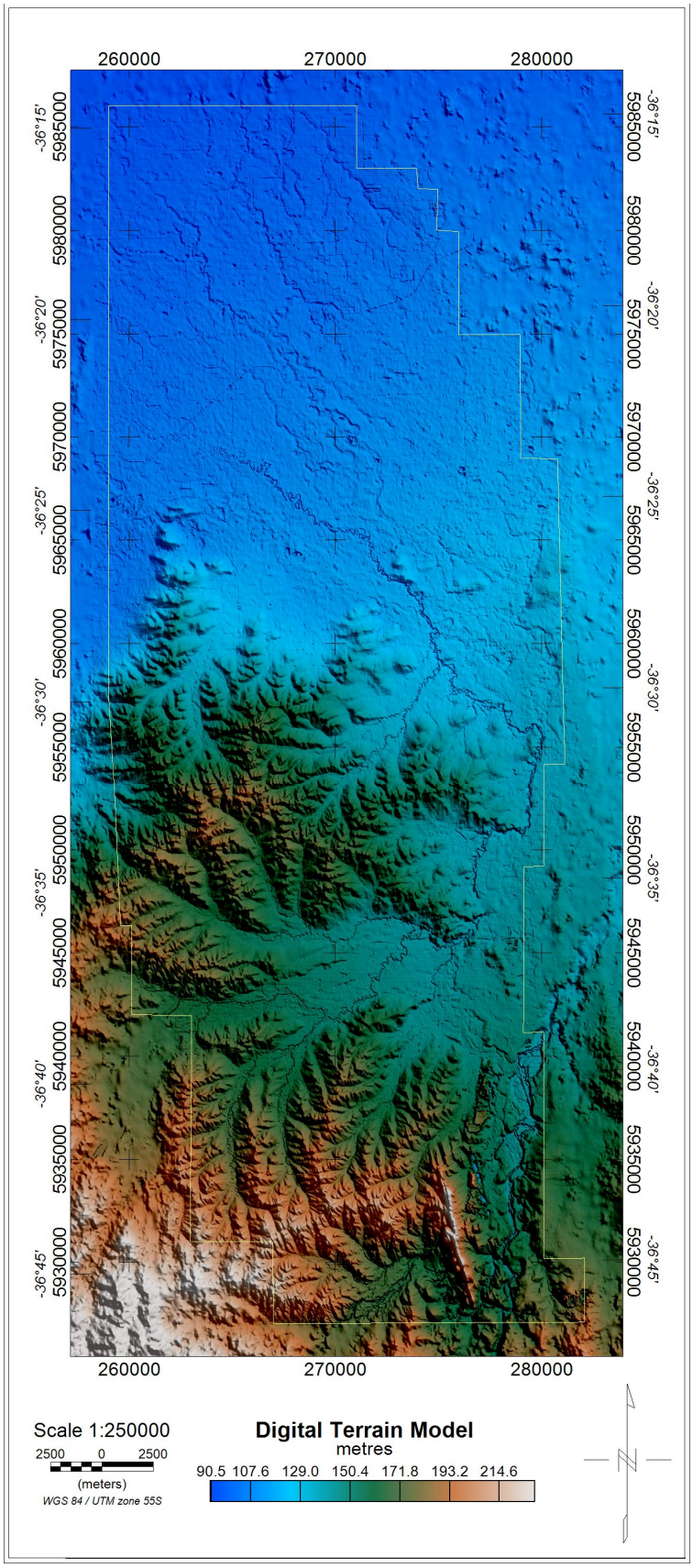


Figure 6: Fosterville – Final Digital Terrain Model (metres, referenced to the EGM96 geoid)

4.6 Terrain Clearance

Terrain clearance for the Fosterville survey averaged above the nominal clearance of 80 m having a mean value of 96.2 m across the survey area. For safety reasons the aircraft flew higher over populated areas in the south of the survey area. The terrain clearance, as derived from laser scanner data, is shown in *Figure 7*.

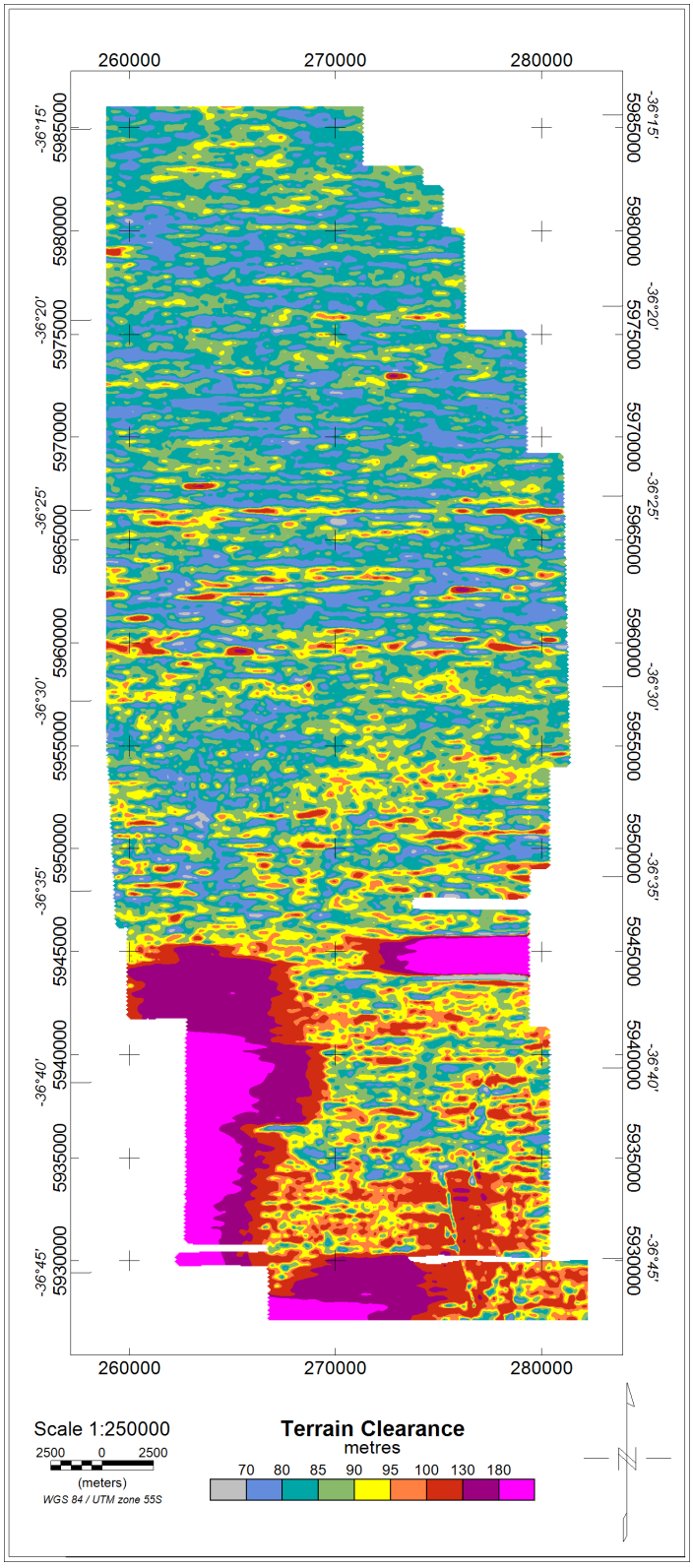


Figure 7: Fosterville – Terrain clearance derived from laser scanner data (metres)

5 FALCON® AIRBORNE GRAVITY GRADIENT (AGG) RESULTS

5.1 Processing Summary

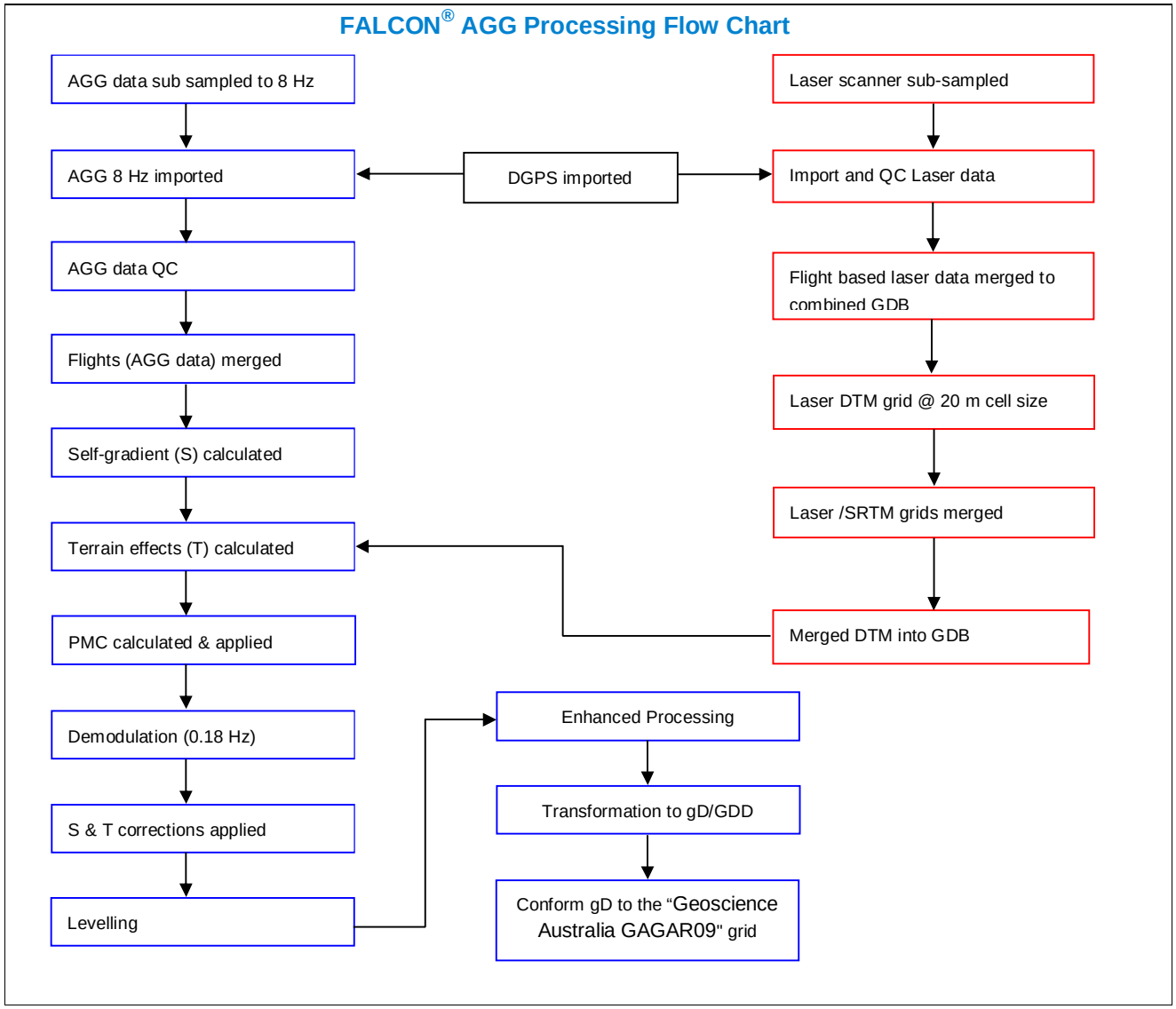


Figure 8: FALCON® AGG Data Processing

5.2 FALCON® Airborne Gravity Gradiometer Data

Figure 8 summarises the steps involved in processing the AGG data obtained from the survey.

The **FALCON®** Airborne Gravity Gradiometer data were digitally recorded by the ADAS on removable hard drives. The raw data were then copied to the field processing laptop, backed up twice onto hard disk media and transferred by Secure File Transfer to the CGG Perth data processing centre.

Preliminary processing and QC of the **FALCON®** AGG data were completed on-site and at the Perth data processing centre using CGG's AGG QC software. Further QC and final **FALCON®** AGG data processing were performed at the Perth data processing centre.

5.3 Radar Altimeter Data

The terrain clearance measured by the radar altimeter in metres was recorded at 10 Hz. The data were plotted and inspected for quality.

5.4 Laser Scanner Data

Laser scanner returns were recorded at a rate of 36 scans per second with each scan returning 276 data points. Each return was converted to ground surface elevation by combining scanner range and angle data with aircraft position and attitude data. Computed elevations were then sub sampled by first dividing each scan into ten segments and combining five adjacent scans per segment, then using a special algorithm to select the optimum return within each data "bin" thus formed. Sub-sampled laser scanner data were edited to remove spikes prior to gridding.

5.5 Positional Data

Differential GPS processing was applied to compute accurate aircraft positions once per second. Waypoint's GrafNav GPS processing software calculated DGPS positions using raw range data obtained from receivers in the aircraft and at a fixed ground base station.

The GPS ground station position was determined by sending several hours of collected data to an online GPS processing service to obtain a differentially corrected computed position. The service selected was AUSPOS, which is provided by Geoscience Australia. The GPS data were processed and quality controlled using the WGS84 datum.

Parameters for the WGS84 datum are:

Ellipsoid: WGS84

Semi-major axis: 6378137.0 m

1/flattening: 298.257

All processing was performed using WGS84/UTM Zone 55S coordinates. Final line data and final grid data were supplied in this projection.

5.6 Terrain Correction

Terrain corrections were derived from the digital terrain model grid for every data point in the survey. A terrain density of 1.00 g/cm^3 was used to compute the terrain correction channels, which were then multiplied by the chosen correction density before being subtracted from the data.

A correction density of 2.67 g/cm^3 was selected as approximating most closely the density of the terrain in the survey area and was applied.

5.7 Mean-Removal Levelling

No tie line data were collected for this survey. The terrain corrected data and the uncorrected data were levelled by removing the mean value for each line.

WARNING: Since levelling is performed after terrain correction, the use of the levelled uncorrected data together with the terrain correction channels to create data corrected for a different terrain density will almost certainly result in residual levelling errors in the new corrected data. An alternative method for computing terrain corrected data for additional densities is described in section *9.11*.

5.8 Micro-levelling

Micro-levelling was applied to the levelled data to remove residual long wavelength levelling errors.

5.9 Enhanced Processing

The enhanced processing technique improves the noise amplitude density (as discussed by Christensen et al, 2015) by 25-50% for surveys with line spacing of less than 1 km. The method exploits the different spatial frequencies of system noise

and geologic signal. After converting the data into the 2D spatial domain, a custom spatial filter is applied that removes the system noise, while retaining the remaining geologic signal. The process will limit the data resolution to the survey line spacing. The Falcon Difference Noise of the standard product is 2.81 E at 333 m resolution and after applying the processing enhancement the Falcon Difference Noise is reduced to 1.23 E at 200 m resolution. Calculating the noise amplitude density is a more appropriate means to evaluate noise with data at different resolutions. The standard product has a noise amplitude density of 1.62 E√km and the enhanced product has a noise amplitude density of 0.55 E√km.

5.10 FALCON® Airborne Gravity Gradient Data - G_{DD} & g_D

The transformation into G_{DD} and g_D was accomplished using the Method of Equivalent Sources.

The equivalent source transformation utilises a smooth model inversion to calculate the density of a surface of sources followed by a forward calculation to produce gD and GDD. It was possible to produce the short to medium wavelength characteristics placing the sources at a depth of 300 metres below the smoothed drape surface (EGM96).

The transformations use a smoothed surface onto which the output data are projected. This surface is a smoother equivalent of the actual flying surface.

The equivalent source (density 2.67 g/cm^3) G_{DD} and g_D maps are shown in Figure 9 and Figure 10 respectively.

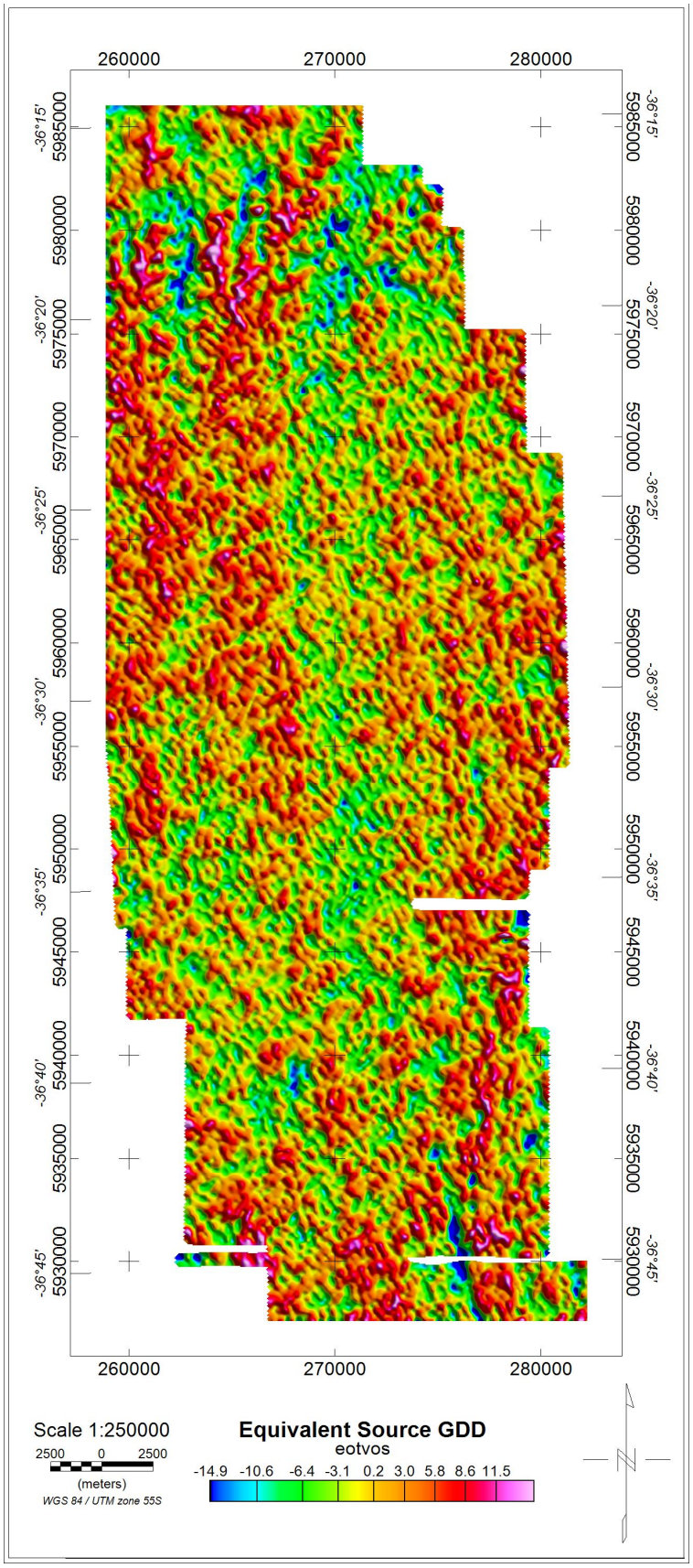


Figure 9: Fosterville – Vertical Gravity Gradient (GDD) from equivalent source processing (eotvos).

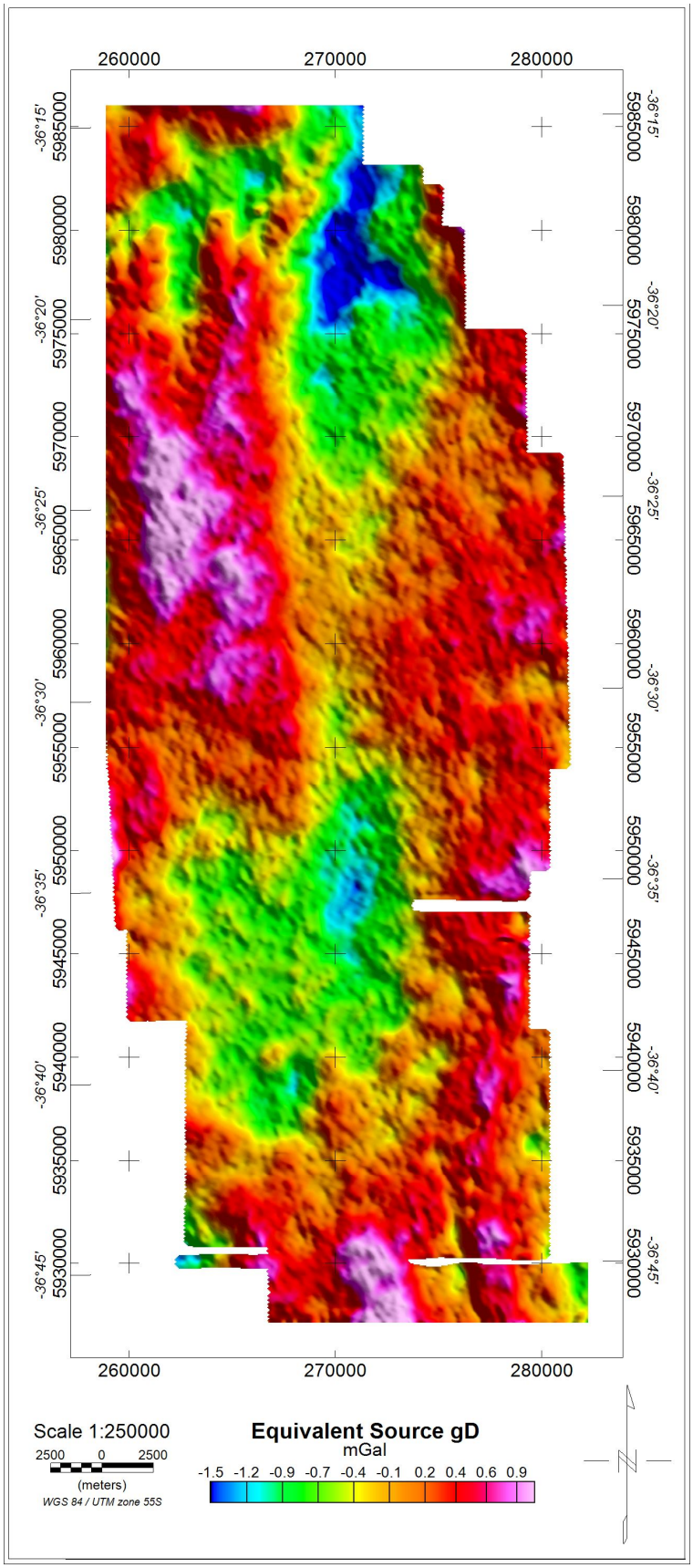


Figure 10: Fosterville – Vertical Gravity (gD) from equivalent source processing (mGal)

5.11 Conforming gD to regional gravity

As discussed in section *9.3*, the long wavelength information in g_D can be improved by incorporating ancillary information. Such information is available in the form of the Geoscience Australia "Gravity Anomaly Grid of the Australian Region (June 2009)" (GAGAR09).

The equivalent source g_D grids were conformed to a subset of the GAGAR09 grid as follows. The (density 2.67 g/cm^3) result is presented in *Figure 11.*

- Low pass filter the regional data using a cosine squared filter with cut-off at 20 km, tapering to 15 km.
- High pass filter the g_D data (Fourier and equivalent source) using a cosine squared filter with cut-off at 20 km, tapering to 15 km.
- Conform the Fourier and equivalent source data to the regional data by addition of the filtered grids. The filter design is such that this method provides uniform frequency response across the overlap frequencies.

Further discussion of this method can be found in Dransfield (2010).

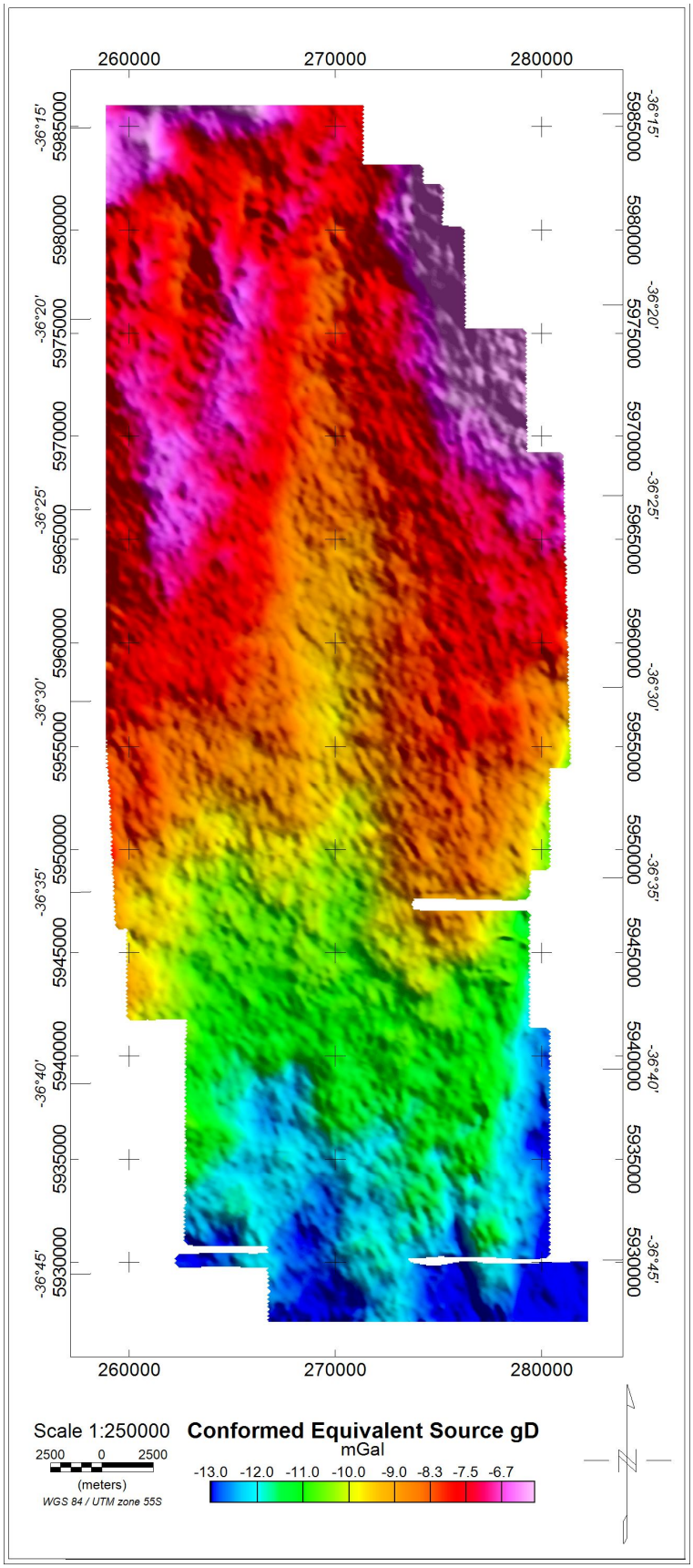


Figure 11: Fosterville – Vertical Gravity (gD) from equivalent source processing conformed to regional gravity data (milligal).

6 MAGNETIC RESULTS

6.1 Processing Summary

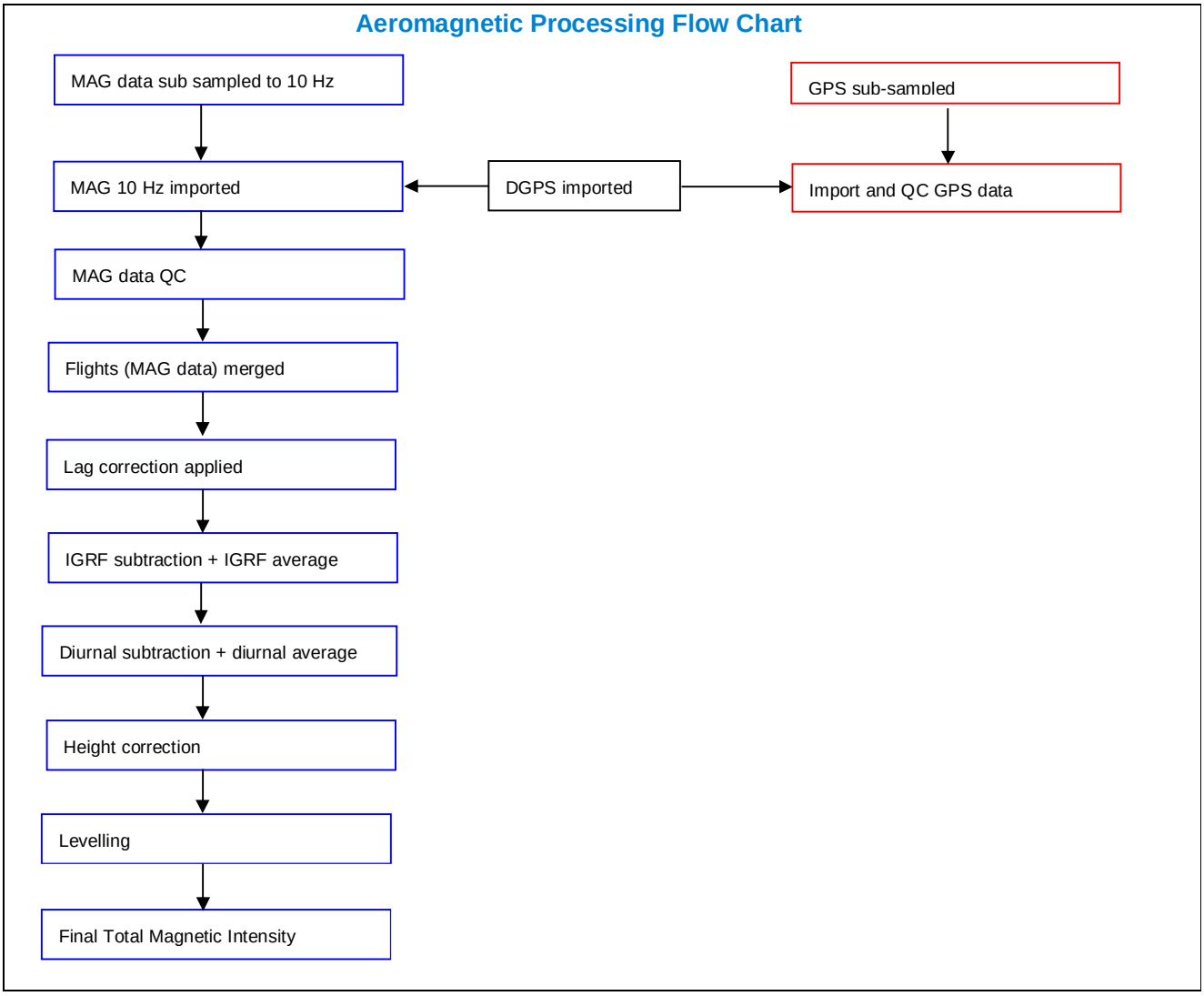


Figure 12: Magnetic Data Processing

6.2 Aeromagnetic Data

Figure 12 summarises the steps involved in processing the aeromagnetic data obtained from the survey.

The aeromagnetic data were digitally recorded by the FASDAS on removable hard drives. The raw data were then copied onto the field processing laptop, backed up twice onto hard drive media and sent via FTP to CGG's secure server.

Preliminary QC of the aeromagnetic data was completed on-site using CGG's proprietary ATLAS software. Further QC and aeromagnetic data processing were performed by the office based data processor.

6.3 Radar Altimeter Data

The terrain clearance measured by the radar altimeter in metres was recorded at 10 Hz. The data were plotted and inspected for quality.

6.4 Positional Data

Refer to section *5.5* for positional data processing.

6.5 Lag Correction

All aeromagnetic data were lagged prior to final processing. A lag of 2.8 seconds was applied.

6.6 IGRF Correction

The IGRF was calculated using the final GPS X, Y and Z positions and this value subtracted from the lag corrected magnetics. A base value of 59379 nT was added back to the magnetics.

6.7 Diurnal Subtraction

The base station magnetics (diurnal) were filtered using a long wavelength filter to retain wavelengths longer than 71 seconds. This value was subtracted from the IGRF corrected total magnetic intensity. Next, based upon the average magnetic value calculated from running the base station for 24 hours, a base value of 59380 nT was added back to the magnetics. This produced the diurnally corrected total magnetic intensity.

6.8 Height Correction

The total magnetic intensity data were height corrected using a differential upward and downward continuation process to the nominal flying height. The laser scanner height (GPS altitude minus DTM) was used for this purpose.

6.9 Micro-levelling

The total magnetic intensity data were micro-levelled using CGG's proprietary ATLAS software.

6.10 Total Magnetic Intensity

The total magnetic intensity has a minimum value of 59138 nT and a maximum value of 59569 nT across the survey area and is presented in *Figure 13*.

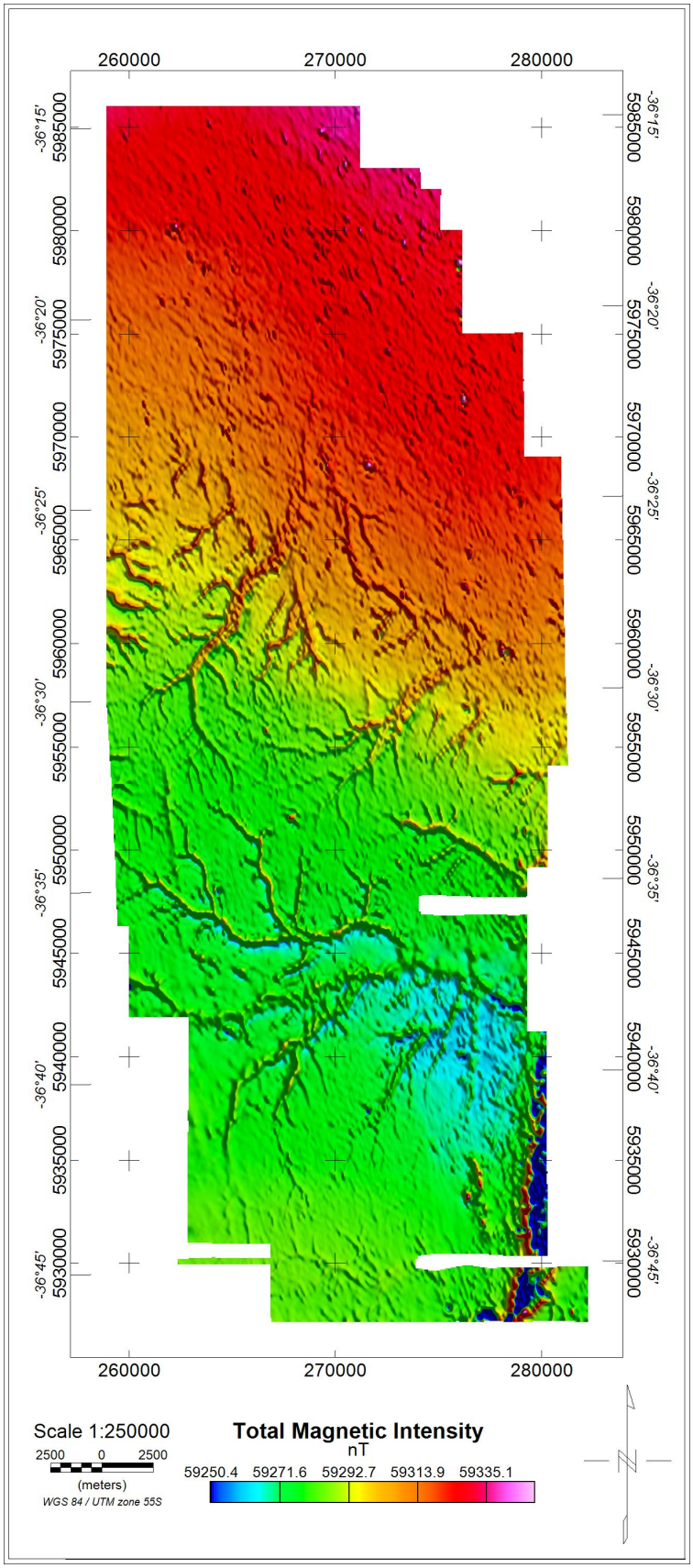


Figure 13: Fosterville – Total Magnetic Intensity (nT)

7 APPENDIX I - SURVEY EQUIPMENT

7.1 Survey Aircraft

A CGG Cessna C208B turbo prop, Australian registration VH-ZKA was used to fly the survey area. The following instrumentation was used for this survey.

7.2 FALCON® Airborne Gravity Gradiometer

FALCON® AGG System (Newton)

The **FALCON®** AGG System is based on current state-of-the-art airborne gravity gradiometer technology and has been optimized for airborne broad band geophysical exploration. The system is capable of supporting surveying activities in areas ranging from 1,000 ft below sea level to 13,000 ft above sea level with aircraft speeds from 30 to 130 knots. The FALCON® AGG data streams were digitally recorded at different rates on removable drives installed in the FALCON® AGG electronics rack.

7.3 Airborne Data Acquisition Systems

Digital Acquisition System (FASDAS)

The FASDAS is a data acquisition system executing propriety software for the acquisition and recording of location, magnetic and ancillary data. Data are presented both numerically and graphically in real time on the VGA display providing on-line quality control capability.

The FASDAS is also used for real time navigation. A pre-programmed flight plan containing boundary coordinates, line start and end coordinates, altitude values calculated for a theoretical drape surface, line spacing and cross track definitions is loaded into the computer prior to each flight. The WGS84 latitude and longitude and altitude received from the real-time corrected, dual frequency Novatel OEMV L1/L2-Band Positioning receiver, is transformed to the local coordinate system for cross track and distance to go values. This information, together with ground heading and speed, is displayed to the pilot numerically and graphically on a two line LCD display. It is also presented on the operator LCD screen in conjunction with a pictorial representation of the survey area, survey lines and ongoing flight path.

FALCON® AGG Data Acquisition System (ADAS)

The FASDAS provides control and data display for the FALCON® AGG system. Data are displayed in real time for the operator and warnings displayed should system parameters deviate from tolerance specifications. All FALCON® AGG and laser scanner data are recorded to a removable hard drive.

7.4 Aerial and Ground Magnetometers

The airborne Caesium magnetometer was a **Scintrex CS-2** having a noise envelope of 0.002 nT pk-pk in 0.01-1 Hz bandwidth.

The ground magnetometer was a **Scintrex CS-2** Caesium sensor sampling at 1 Hz.

7.5 Real-Time Differential GPS

The **Novatel OEMV L-band** positioning receiver provides real-time differential GPS for the on-board navigation system. The differential data set was relayed via a geo-synchronous satellite to the aircraft where the receiver optimized the corrections for the current location.

7.6 GPS Base Station Receiver

The **Javad Triumph-1** GPS receiver is a 216 channel multi-frequency GPS receiver. It can provide raw range information of all satellites in view from the GPS, GLONASS, BeiDou and Galileo satellite systems. The receiver can sample at up to 5 Hz and records to internal memory. These data are post-processed with the rover data to provide differential GPS (DGPS) corrections for the flight path.

7.7 Altimeters

Collins Alt-50 Radar Altimeter

The radar altimeter has an accuracy of 2 ft or +/-2%, a range of 0-2,000 ft and a measurement rate of 10 Hz. Altimeter data were used for flying but were not a deliverable product.

7.8 Laser Scanner

Riegl LMS-Q240I-60

The laser scanner is designed for high speed line scanning applications. The system is based upon the principle of time-of-flight measurement of short laser pulses in the infrared wavelength region and the angular deflection of the laser beam is obtained by a rotating polygon mirror wheel. The measurement range is up to 650 m with a minimum range of 2 m and an accuracy of 20 mm. The laser beam is eye safe, the laser wavelength is 0.9 μm, the scan angle range is +/- 40° and the scan speed is 36 scans/s.

7.9 Data Processing Hardware and Software

The following equipment and software were used:

Hardware

- One 2.0 GHz (or higher) laptop computer
- External USB hard drive reader for ADAS removable drives
- Two External USB hard drives for data backup
- All-In-One printer, copier, scanner

Software

- Oasis Montaj data processing and imaging software
- GrafNav Differential GPS processing software
- CGG - Atlas data processing software
- CGG - DiAGG processing software

8 APPENDIX II - SYSTEM TESTS

8.1 Instrumentation Lag

Due to the relative position of the magnetometer, altimeters and GPS antenna on the aircraft and to processing/recording time lags, raw readings from each data stream vary in position. To correct for this and to align selected anomaly features on lines flown in opposite directions, the magnetic and altimeter data are 'parallaxed' with respect to the position information. The lags were applied to the data during processing.

8.2 Radar Altimeter Calibration

The radar altimeter is checked for accuracy and linearity every 12 months, or when any change in a key system component requires this procedure to be carried out. This calibration allows the radar altimeter data to be compared and assessed with the other height data (GPS, barometric and laser) to confirm the accuracy of the radar altimeter over its operating range. The calibration is performed by flying a number of 30 second lines at preselected terrain clearances over an area of flat terrain and using the results of the radar altimeter, differentially corrected GPS heights in mean sea level (MSL) and laser scanner were used to derive slope and offset information.

8.3 Magnetometer Compensation

The magnetometer compensation corrects the magnetometer readings for the effect of the magnetic field of the aircraft, both static and dynamic, on the readings.

The compensation correction is calculated using a fluxgate magnetometer to measure the aircraft's manoeuvres. Manoeuvres consist of +/-5 degree rolls, +/-10 degree pitches and +/-5 degree yaws peak to peak over periods of 5 seconds repeated in each line direction. The magnetometer compensation is repeated when a change big enough to impact on the magnetometer has been made to the aircraft or its contents. A magnetometer compensation is normally performed in an area with similar magnetic declination, inclination and field strength to the survey area i.e. close to or within the survey area.

8.4 FALCON® AGG Noise Measurement

At the commencement of the survey, 20 minutes of data were collected with the aircraft in straight level flight at 3500 ft AGL. These data were assessed in-flight to check the AGG noise levels.

Daily flight debriefs incorporating **FALCON®** AGG performance statistics for each flight line are prepared using output from CGG DiAGG software. These are sent daily to CGG office staff for performance evaluation.

8.5 Daily Calibrations

A set of daily calibrations were performed each survey day as follows:

- Magnetic base station time check
- AGG Quiescent Calibration

8.5.1 Magnetic Base Station Time Check

Prior to each day's survey all magnetic base stations were synchronised using broadcast GPS time signals.

8.5.2 FALCON® AGG Calibration

A calibration was performed at the beginning of each flight and the results monitored by the operator. The coefficients obtained from each of the calibrations were used in the processing of the data.

9 APPENDIX III - FALCON® AGG DATA & PROCESSING

9.1 Nomenclature

The **FALCON®** airborne gravity gradiometer (AGG) system adopts a North, East, and Down coordinate sign convention and these directions (N, E, and D) are used as subscripts to identify the gravity gradient tensor components (gravity vector derivatives). Lower case is used to identify the components of the gravity field and upper case to identify the gravity gradient tensor components. Thus the parameter usually measured in a normal exploration ground gravity survey is $\mathbf{g_D}$ and the vertical gradient of this component is $\mathbf{G_{DD}}$.

9.2 Units

The vertical component of gravity ($\mathbf{g_D}$) is delivered in the usual units of mGal. The gradient tensor components are delivered in eotvos, which is usually abbreviated to "E". By definition **1 E = 10^{-4} mGal/m.**

9.3 FALCON® Airborne Gravity Gradiometer Surveys

In standard ground gravity surveys, the component measured is "$\mathbf{g_D}$", which is the *vertical component of the acceleration due to gravity*. In airborne gravity systems, since the aircraft is itself accelerating, measurement of "$\mathbf{g_D}$" cannot be made to the same precision and accuracy as on the ground. Airborne gravity gradiometry uses a differential measurement to remove the aircraft motion effects and delivers gravity data of a spatial resolution and sensitivity comparable with ground gravity data.

The **FALCON®** gradiometer instrument acquires two curvature components of the gravity gradient tensor namely $\mathbf{G_{NE}}$ and $\mathbf{G_{UV}}$ where $\mathbf{G_{UV}} = (\mathbf{G_{NN}} - \mathbf{G_{EE}})/2$.

A feature of the **FALCON®** AGG system is that two independent measurements are made of both the NE and UV curvature components. This is achieved by using two sets of accelerometers, referred to as the A complement and the B complement. Each complement consists of four accelerometers. The measured gradients from these complements are referred to as A_{NE} and A_{UV} and B_{NE} and B_{UV}. The $\mathbf{G_{NE}}$ and $\mathbf{G_{UV}}$ gradients are computed by averaging A and B:

$$\boldsymbol{G_{NE}} = \frac{(A_{NE} + B_{NE})}{2}$$

$$\boldsymbol{G_{UV}} = \frac{(A_{UV} + B_{UV})}{2}$$

Since these curvature components cannot easily and intuitively be related to the causative geology, they are transformed into the vertical gravity gradient ($\mathbf{G_{DD}}$), and integrated to derive the vertical component of gravity ($\mathbf{g_D}$). Interpreters display, interpret and model both $\mathbf{G_{DD}}$ and $\mathbf{g_D}$. The directly measured $\mathbf{G_{NE}}$ and $\mathbf{G_{UV}}$ data are appropriate for use in inversion software to generate density models of the earth. The vertical gravity gradient, $\mathbf{G_{DD}}$, is more sensitive to small or shallow sources and has greater spatial resolution than $\mathbf{g_D}$ (similar to the way that the vertical magnetic gradient provides greater spatial resolution and increased sensitivity to shallow sources of the magnetic field). In the integration of $\mathbf{G_{DD}}$ to give $\mathbf{g_D}$, the very long wavelength component, at wavelengths comparable to or greater than the size of the survey area, cannot be fully recovered. Long wavelength gravity are therefore incorporated in the $\mathbf{g_D}$ data from other sources. This might be regional ground, airborne or marine gravity if such data are available. The Danish Technical University global gravity data of 2013 (DTU13) are used as a default if other data are not available.

9.4 Gravity Data Processing

The main elements and sequence of processing of the gravity data are given below. Unless not applicable or specified otherwise, the processing step is applied to each individual complement element (A_{NE}, A_{UV}, B_{NE}, B_{UV}):

1. Dynamic corrections for residual aircraft motion (called Post Mission Compensation or PMC) are calculated and applied.
2. Self-gradient corrections are calculated and applied to reduce the time-varying gradient response from the aircraft and platform.
3. A Digital Terrain Model (DTM) is created from the laser scanner range data, the AGG inertial navigation system rotation data and the DGPS position data.
4. Terrain corrections are calculated and applied.
5. Tie line levelling and micro-levelling (where necessary) are applied.
6. $\mathbf{G_{NE}}$ and $\mathbf{G_{UV}}$ are transformed into the full gravity gradient tensor, including $\mathbf{G_{DD}}$, and into $\mathbf{g_D}$.

9.5 Aircraft Dynamic Corrections

The design and operation of the **FALCON**® AGG results in very considerable reduction of the effects of aircraft acceleration but residual levels are still significant and further reduction is required and must be done in post-processing.

Post-processing correction relies on monitoring the inertial acceleration environment of the gravity gradiometer instrument (GGI) and constructing a model of the response of the GGI to this environment. Parameters of the model are adjusted by regression to match the sensitivity of the GGI during data acquisition. The modelled GGI output in response to the inertial sensitivities is subtracted from the observed output. Application of this technique to the output of the GGI, when it is adequately compensated by its internal mechanisms, reduces the effect of aircraft motion to acceptable levels.

Following these corrections, the gradient data are demodulated and filtered along line using a 6-pole Butterworth low-pass filter with a cut-off frequency of 0.18 Hz.

9.6 Self-gradient Corrections

The GGI is mounted in gimbals controlled by an inertial navigation system which keeps the GGI pointing in a fixed direction whilst the aircraft and gimbals rotate around it. Consequently, the GGI measures a time-varying gravity gradient due to these masses moving around it as the heading and attitude of the aircraft changes during flight. This is called the self-gradient.

Like the aircraft dynamic corrections, the self-gradient is calculated by regression of model parameters against measured data. In this case, the rotations of the gimbals are the input variables of the model. Once calculated, the modelled output is subtracted from the observed output.

9.7 Laser Scanner Processing

The laser scanner measures the range from the aircraft to the ground in a swath of angular width ±40 degrees below the aircraft. The aircraft attitude (roll, pitch and heading) data provided by the AGG inertial navigation system are used to adjust the range data for changes in attitude and the processed differential GPS data are used to reference the range data to located ground elevations referenced to the WGS84 datum (corrected for the EGM96 geoid separation model). Statistical filtering strategies are used to remove anomalous elevations due to foliage or built up environment. The resulting elevations are gridded to form a digital terrain model (DTM).

9.8 Terrain Corrections

An observation point above a hill has excess mass beneath it compared to an observation point above a valley. Since gravity is directly proportional to the product of the masses, uncorrected gravity data have a high correlation with topography.

It is therefore necessary to apply a terrain correction to gravity survey data. For airborne gravity gradiometry at low survey heights, a detailed DTM is required. Typically, immediately below the aircraft, the digital terrain will need to be sampled at a cell size roughly one-third to one-half of the survey height and with a position accuracy of better than 1 metre. For these accuracies, LIDAR data are required and each **FALCON**® survey aircraft comes equipped with LIDAR (laser scanner).

If bathymetric data are used then these form a separate terrain model for which terrain corrections are calculated at a density chosen to suit the water bottom – water interface.

Once the DTM has been merged, the terrain corrections for each of the $\mathbf{G_{NE}}$ and $\mathbf{G_{UV}}$ data streams are calculated. In the calculation of terrain corrections, a density of 1 g/cm^3 is used. The calculated corrections are stored in the database allowing the use of any desired terrain correction density by subtracting the product of desired density and correction from the measured $\mathbf{G_{NE}}$ and $\mathbf{G_{UV}}$ data. The terrain correction density is chosen to be representative of the terrain density over the survey area. Sometimes more than one density is used with input from the client.

Typically, the terrain corrections are calculated over a distance 40 to 60 km from each survey measurement point.

9.9 Tie line Levelling

The terrain and self-gradient corrected $\mathbf{G_{NE}}$ and $\mathbf{G_{UV}}$ data are tie line levelled across the entire survey using a least-squares minimisation of differences at survey line intersections. Occasionally some micro-levelling might be performed.

9.10 Transformation into GDD & g_D

The transformation of the measured, corrected and levelled $\mathbf{G_{NE}}$ and $\mathbf{G_{UV}}$ data into gravity and components of the full gravity gradient tensor is accomplished using two methods:

- Fourier domain transformation
- Equivalent source transformation

The input data for the Fourier method are the average **NE** and **UV** components computed from the complement data, as described in section *9.3*. The Fourier method relies on the Fourier transform of Laplace's equation. The application of this transform to the complex function $\mathbf{G_{NE} + i\, G_{UV}}$ provides a stable and accurate calculation of each of the full tensor components and gravity. The Fourier method performs piece-wise upward and downward continuation to work with data collected on a surface that varies from a flat horizontal plane. For stability of the downward continuation, the data are low-pass filtered. The cut-off wavelength of this filter depends on the variations in altitude range and line spacing. It is set to the smallest value that provides stable downward continuation.

In survey areas where the variability of the terrain surface (and hence the flight surface) makes it impossible to obtain Fourier transformation results that are both high resolution and stable, an alternate method can be applied which bypasses the upward and downward continuation steps. The results are calculated at the flight surface. This approach lacks the mathematical rigour of the complete method but allows for greater detail in the output data. It must be noted however that, if the terrain is too extreme, this method may fail to accurately transform the input data. This can be checked by comparing the input GNE and GUV data with the predicted values of the same data after transformation. If they do not match well, the Fourier transformation method cannot be relied upon.

The input data for the equivalent source method are the individual **NE** and **UV** component data from each complement, as referred to in section *9.3*. The equivalent source method relies on a smooth model inversion to calculate the density of a surface of sources and from these sources, a forward calculation provides the $\mathbf{G_{DD}}$ and $\mathbf{g_D}$ data as well as the other gradient tensor components. The effect of the smoothing is similar to but not the same as the application of the low-pass filter in the Fourier domain method. In areas of highly variable terrain, flying low can lead to some instability in the equivalent source method as the computation surface approaches the location of the derived sources. It may be necessary to accept some localised instability in order to optimise the overall result.

The equivalent source procedure defines an array of rectangular (usually square) plates, extending slightly past the survey area in all directions. Each plate is assumed to have uniform (but initially unknown) surface density and to lie on a predefined solution surface. Using the individual NE and UV component data measured at the centre of each plate, a system of linear equations is formed which can then be solved for the density of each plate using a least squares inversion method. Once the plate density distribution is determined, it can be used for forward calculation of all tensor components and of vertical gravity.

The limitations of gravity gradiometry in reconstructing the long wavelengths of gravity can lead to differences in the results of these two methods at long wavelength. The merging of the $\mathbf{g_D}$ data with externally supplied regional gravity such as the DNSC08 gravity provides a way of reducing these differences. The application of this procedure will depend on the survey size and resolution of available regional gravity. If survey size is too small or regional gravity resolution too large, regional conforming is not applied.

9.11 Terrain Corrections Using Alternate Terrain Densities

Although both uncorrected processed and transformed data and unit density terrain correction data are supplied, it is not recommended that these be used to create final data corrected for any arbitrary terrain correction density. The principal reason for this is that tie line levelling occurs after application of the terrain correction. As a result, levelling errors present in the terrain correction channels by virtue of positional inaccuracy are not removed from these channels and will be present in any data corrected with them. Further, filtering applied in creating the uncorrected, transformed data is not applied to the terrain correction channels. Mixing data filtered in different ways is not advised.

An alternative method (valid only for datasets where waterbody(ies) have not been taken into account when computing the terrain corrections) uses the linear relationship between the terrain corrections at different densities and the corresponding gravity gradient or $\mathbf{g_D}$ values. This method can be applied to either the grid data or the located data. An example is given using $\mathbf{G_{DD}}$:

The new density is referred to as ρ_N, the existing densities as ρ_1 and ρ_2

$$G_{DD}(\rho_N) = G_{DD}(\rho_1) + \left(G_{DD}(\rho_2) - G_{DD}(\rho_1)\right) \times \frac{(\rho_N - \rho_1)}{(\rho_2 - \rho_1)}$$

Note that the terrain correction channel is eliminated by substitution in deriving this equation.

It is recommended that two densities that differ by a reasonable value be used for this method, in order to minimise uncertainties caused by noise in the data. The values of 0.00 and 2.67 g/cm^3 usually delivered should be sufficient to yield useful results.

When the effect of waterbodies are included in deriving the terrain corrections (bathymetry data have been supplied, enabling the creation of a combined bathymetry and elevation grid to be used for the terrain correction); an alternative method is required. This method requires waterbody corrected gradients, or $\mathbf{g_D}$, as part of the equation, rather than the ρ_1 data.

The new density is referred to as ρ_N, the existing density is ρ_2 and *WB* refers to the supplied waterbody corrected data.

$$G_{DD}(\rho_N) = G_{DD_{WB}} + \left(G_{DD}(\rho_2) - G_{DD_{WB}}\right) \times \frac{(\rho_N)}{(\rho_2)}$$

9.12 Noise & Signal

By taking two independent measurements of the NE and UV curvature components at each sample point, it is possible to obtain a direct indication of the reliability of these measurements. The standard deviation of half the difference of the pairs of measurements - (A_{NE},B_{NE}) and (A_{UV},B_{UV}) - provides a good estimate of the survey noise:

$$Noise_{NE} = StdDev\left(\frac{(A_{NE} - B_{NE})}{2}\right)$$

$$Noise_{UV} = StdDev\left(\frac{(A_{UV} - B_{UV})}{2}\right)$$

These difference channels are calculated for each data point. The standard deviation across all data points is the figure quoted for the survey as a whole.

This difference error has been demonstrated to follow a 'normal' or Gaussian statistical distribution, with a mean of zero. Therefore, the bulk of the population (95%) will lie between -2σ and +2σ of the mean. For a typical survey noise estimate of, say, 3 E, 95% of the noise will be between -6 E and +6 E.

These typical errors in the curvature gradients translate to errors in $\mathbf{G_{DD}}$ of about 5 E and in $\mathbf{g_D}$ (in the shorter wavelengths) in the order of 0.1 mGal.

9.13 Risk Criteria in Interpretation

The risks associated with a **FALCON**® AGG survey are mainly controlled by the following factors.

- **Survey edge anomalies** – the transformation from measured curvature gradients to vertical gradient and vertical gravity gradient is subject to edge effects. Hence any anomalies located within about 2 x line spacing of the edge of the survey boundaries should be treated with caution.
- **Single line anomalies** – for a wide-spaced survey, an anomaly may be present on only one line. Although it might be a genuine anomaly, the interpreter should note that no two-dimensional control can be applied.
- **Low amplitude (less than 2σ) anomalies** – Are within the noise envelope and need to be treated with caution, if they are single line anomalies and close in diameter to the cut-off wavelengths used.
- **Residual topographic error anomalies** – Inaccurate topographic correction either due to inaccurate DTM or local terrain density variations may produce anomalies. Comparing the DTM with the G_{DD} map terrain-corrected for different densities is a reliable way to confirm the legitimacy of an anomaly.
- **The low density of water and lake sediments** – (if present) can create significant gravity and gravity gradient lows which may be unrelated to bedrock geology. It is recommended that all anomalies located within lakes or under water be treated with caution and assessed with bathymetry if available.

9.14 References

Boggs, D. B. and Dransfield, M. H., 2004, Analysis of errors in gravity derived from the Falcon® airborne gravity gradiometer, Lane, R. (ed.), Airborne Gravity 2004 - Abstracts from the ASEG-PESA Airborne Gravity 2004 Workshop, Geoscience Australia Record 2004/18, 135-141.

Christensen A.N., Dransfield, M. H. and Van Galder C, 2015, Noise and repeatability of airborne gravity gradiometry, First Break, Volume 33, April 2015, 55 - 63.

Dransfield, M. H., 2010, Conforming Falcon gravity and the global gravity anomaly, Geophysical Prospecting, 58, 469-483.

Dransfield, M. H. and Lee, J. B., 2004, The FALCON® airborne gravity gradiometer survey systems, Lane, R. (ed.), Airborne Gravity 2004 - Abstracts from the ASEG-PESA Airborne Gravity 2004 Workshop, Geoscience Australia Record 2004/18, 15-19.

Dransfield, M. H. and Zeng, Y., Airborne gravity gradiometry: terrain corrections and elevation error, Geophysics 2009/Sep 74(5).

Lee, J. B., 2001, FALCON Gravity Gradiometer Technology, Exploration Geophysics, 32, 75-79.

Lee, J. B.; Liu, G.; Rose, M.; Dransfield, M.; Mahanta, A.; Christensen, A. and Stone, P., 2001, High resolution gravity surveys from a fixed wing aircraft, Geoscience and Remote Sensing Symposium, 2001. IGARSS '01. IEEE 2001 International, 3, 1327-1331.

Stone, P. M. and Simsky, A., 2001, Constructing high resolution DEMs from Airborne Laser Scanner Data, Preview, Extended Abstracts: ASEG 15th Geophysical Conference and Exhibition, August 2001, Brisbane, 93, 99.

10 APPENDIX IV - FINAL PRODUCTS

Final **FALCON**® AGG digital line data were provided in a Geosoft Oasis GDB database files containing the fields and format described in *Table 4* below.

Final magnetic digital line data were provided in a Geosoft Oasis GDB database files containing the fields and format described in *Table 5* below.

Grids of equivalent source products, total magnetic intensity and the DTM were delivered, as described in *Table 6* below. The grids are in ERMapper ERS formats with a 50 m cell size, with the exception of the DTM grid which has a 20 m cell size.

One copy of the digital archives was delivered along with a hard copy of this Logistics and Processing Report.

Field	Variable	Description	Units
1	Line	Line number	
2	Flight	Flight number	
3	Date_Local	Local flight date Gregorian calendar (YYYYMMDD)	yyyymmdd
4	Time_SSM_UTC1980	Universal Time (Seconds from the start of the 6th of January 1980 without Leap Seconds)	seconds
5	Time_SSM_UTC	Universal Time (seconds since midnight)	seconds
6	GNSS_Easting_WGS84 UTM55	WGS84UTM55 easting of the GNSS antenna observation	metres
7	GNSS_Northing_WGS84 UTM55	WGS84UTM55 northing of the GNSS antenna observation	metres
8	GNSS_Longitude_WGS8 4	Observed WGS84 longitude of the GNSS antenna	degrees
9	GNSS_Latitude_WGS84	Observed WGS84 latitude of the GNSS antenna	degrees
10	Elevation_GNSS_GRS8 0	Observed GRS80 ellipsoid elevation of the GNSS antenna	metres
11	Elevation_GNSS_MSL	Observed EGM96 geoid elevation of the GNSS antenna (after application of undulation correction to GRS80 elevation data)	metres
12	Ground_Clearance_GGI _TCGrid_DSM_MSL	Clearance of the GGI above the Digital Surface Model (TCGrid_DSM_MSL) derived from the GGI elevation (MSL)	metres
13	TCGrid_DSM_MSL	Sampled from the Digital Surface Model (DSM) that was used for gravity terrain corrections	metres
14	Turbulence	Vertical acceleration from the AGG Instrument band-pass filtered between 0.3 and 10 Hz (vertical acceleration where g	millig
15	Diff_AmB_NE_2p67_0p1 8HzLP	(A_NE - B_NE)/2 where A and B complement data have been demodulated corrected for dynamic effects (PMC) subject to a 0.18Hz low-pass filter (Demod filtered) self-gradient corrected and terrain corrected with a density of 2.67 t/m^3	Eotvos
16	Diff_AmB_UV_2p67_0p1 8HzLP	(A_UV - B_UV)/2 where A and B complement data have been demodulated corrected for dynamic effects (PMC) subject to a 0.18Hz low-pass filter (Demod filtered) self-gradient corrected and terrain corrected with a density of 2.67 t/m^3	Eotvos
17	Falc_Corr_TC_DD_1p00 _0p18HzLP_TCGrid_DS M_MSL	Terrain effect for DD gravity gradient 0.18Hz low-pass filtered for the observed aircraft vertical location for a density of 1 t/m^3 using the Digital Surface Model	Eotvos
18	Falc_Corr_TC_NE_1p00 _0p18HzLP_TCGrid_DS M_MSL	Terrain effect for NE gravity gradient 0.18Hz low-pass filtered for the observed aircraft vertical location for a density of 1 t/m^3 using the Digital Surface Model	Eotvos
19	Falc_Corr_TC_UV_1p00 _0p18HzLP_TCGrid_DS M_MSL	Terrain effect for UV gravity gradient 0.18Hz low-pass filtered for the observed aircraft vertical location for a density of 1 t/m^3 using the Digital Surface Model	Eotvos
20	Falc_A_NE_0p00_0p18 Hz_MeanLev	A complement NE component demodulated corrected for dynamic effects (PMC) subject to a minimum 0.18Hz low-pass filter (Demod filtered) self-gradient corrected terrain corrected with a density of 0.00 t/m^3 and mean levelled	Eotvos

21	Falc_A_UV_0p00_0p18Hz_MeanLev	A complement UV component demodulated corrected for dynamic effects (PMC) subject to a minimum 0.18Hz low-pass filter (Demod filtered) self-gradient corrected terrain corrected with a density of 0.00 t/m^3 and mean levelled	Eotvos
22	Falc_B_NE_0p00_0p18Hz_MeanLev	B complement NE component demodulated corrected for dynamic effects (PMC) subject to a minimum 0.18Hz low-pass filter (Demod filtered) self-gradient corrected terrain corrected with a density of 0.00 t/m^3 and mean levelled	Eotvos
23	Falc_B_UV_0p00_0p18Hz_MeanLev	B complement UV component demodulated corrected for dynamic effects (PMC) subject to a minimum 0.18Hz low-pass filter (Demod filtered) self-gradient corrected terrain corrected with a density of 0.00 t/m^3 and mean levelled	Eotvos
24	Falc_A_NE_2p67_0p18Hz_MeanLev	A complement NE component demodulated corrected for dynamic effects (PMC) subject to a minimum 0.18Hz low-pass filter (Demod filtered) self-gradient corrected terrain corrected with a density of 2.67 t/m^3 and mean levelled	Eotvos
25	Falc_A_UV_2p67_0p18Hz_MeanLev	A complement UV component demodulated corrected for dynamic effects (PMC) subject to a minimum 0.18Hz low-pass filter (Demod filtered) self-gradient corrected terrain corrected with a density of 2.67 t/m^3 and mean levelled	Eotvos
26	Falc_B_NE_2p67_0p18Hz_MeanLev	B complement NE component demodulated corrected for dynamic effects (PMC) subject to a minimum 0.18Hz low-pass filter (Demod filtered) self-gradient corrected terrain corrected with a density of 2.67 t/m^3 and mean levelled	Eotvos
27	Falc_B_UV_2p67_0p18Hz_MeanLev	B complement UV component demodulated corrected for dynamic effects (PMC) subject to a minimum 0.18Hz low-pass filter (Demod filtered) self-gradient corrected terrain corrected with a density of 2.67 t/m^3 and mean levelled	Eotvos
28	Smooth_Drape_Surface_MSL	Smooth Drape Surface on MSL (EGM96) datum for gravity data reconstruction by the Equivalent Source method	metres
29	Falc_gD_0p00_0p18HzLP_ESD300m_SD	Equivalent Source (300m below drape) derived gD vertical gravity with 0.18Hz low pass line data filtering without terrain correction gridded and reconstructed on the Smooth Drape Surface	mGal
30	Falc_GDD_0p00_0p18HzLP_ESD300m_SD	Equivalent Source (300m below drape) derived GDD vertical gravity gradient with 0.18Hz low pass line data filtering without terrain correction gridded and reconstructed on the Smooth Drape Surface	Eotvos
31	Falc_GED_0p00_0p18HzLP_ESD300m_SD	Equivalent Source (300m below drape) derived GED gravity gradient with 0.18Hz low pass line data filtering without terrain correction gridded and reconstructed on the Smooth Drape Surface	Eotvos
32	Falc_GEE_0p00_0p18HzLP_ESD300m_SD	Equivalent Source (300m below drape) derived GEE gravity gradient with 0.18Hz low pass line data filtering without terrain correction gridded and reconstructed on the Smooth Drape Surface	Eotvos
33	Falc_GND_0p00_0p18HzLP_ESD300m_SD	Equivalent Source (300m below drape) derived GND gravity gradient with 0.18Hz low pass line data filtering without terrain correction gridded and reconstructed on the Smooth Drape Surface	Eotvos
34	Falc_GNN_0p00_0p18HzLP_ESD300m_SD	Equivalent Source (300m below drape) derived GNN gravity gradient with 0.18Hz low pass line data filtering without terrain correction gridded and reconstructed on the Smooth Drape Surface	Eotvos
35	Falc_GNE_0p00_0p18HzLP_ESD300m_SD	Equivalent Source (300m below drape) derived GNE gravity gradient with 0.18Hz low pass line data filtering without terrain correction gridded and reconstructed on the Smooth Drape Surface	Eotvos
36	Falc_GUV_0p00_0p18HzLP_ESD300m_SD	Equivalent Source (300m below drape) derived GUV gravity gradient with 0.18Hz low pass line data filtering without terrain correction gridded and reconstructed on the Smooth Drape Surface	Eotvos

37	Falc_gD_2p67_0p18HzLP_ESD300m_SD	Equivalent Source (300m below drape) derived gD vertical gravity with 0.18Hz low pass line data filtering with terrain correction with density contrast of 2.67t/m^3 gridded 0.5km low-pass grid filtered and reconstructed on the Smooth Drape Surface	mGal
38	Falc_GDD_2p67_0p18HzLP_ESD300m_SD	Equivalent Source (300m below drape) derived GDD vertical gravity gradient with 0.18Hz low pass line data filtering with terrain correction with density contrast of 2.67t/m^3 gridded and reconstructed on the Smooth Drape Surface	Eotvos
39	Falc_GED_2p67_0p18HzLP_ESD300m_SD	Equivalent Source (300m below drape) derived GED gravity gradient with 0.18Hz low pass line data filtering with terrain correction with density contrast of 2.67t/m^3 gridded and reconstructed on the Smooth Drape Surface	Eotvos
40	Falc_GEE_2p67_0p18HzLP_ESD300m_SD	Equivalent Source (300m below drape) derived GEE gravity gradient with 0.18Hz low pass line data filtering with terrain correction with density contrast of 2.67t/m^3 gridded and reconstructed on the Smooth Drape Surface	Eotvos
41	Falc_GND_2p67_0p18HzLP_ESD300m_SD	Equivalent Source (300m below drape) derived GND gravity gradient with 0.18Hz low pass line data filtering with terrain correction with density contrast of 2.67t/m^3 gridded and reconstructed on the Smooth Drape Surface	Eotvos
42	Falc_GNN_2p67_0p18HzLP_ESD300m_SD	Equivalent Source (300m below drape) derived GNN gravity gradient with 0.18Hz low pass line data filtering with terrain correction with density contrast of 2.67t/m^3 gridded and reconstructed on the Smooth Drape Surface	Eotvos
43	Falc_GNE_2p67_0p18HzLP_ESD300m_SD	Equivalent Source (300m below drape) derived GNE gravity gradient with 0.18Hz low pass line data filtering with terrain correction with density contrast of 2.67t/m^3 gridded and reconstructed on the Smooth Drape Surface	Eotvos
44	Falc_GUV_2p67_0p18HzLP_ESD300m_SD	Equivalent Source (300m below drape) derived GUV gravity gradient with 0.18Hz low pass line data filtering with terrain correction with density contrast of 2.67t/m^3 gridded and reconstructed on the Smooth Drape Surface	Eotvos

Table 4: Final FALCON® AGG Digital Data – Geosoft Database Format

Field	Variable	Description	Units
1	Line	Line Number	
2	Flight	Flight Number	
3	Date_Local	Local flight date Gregorian calendar (YYYYMMDD)	yyyymmdd
4	Time_SSM_UTC1980	Universal Time (Seconds from the start of the 6th of January 1980 without Leap Seconds)	seconds
5	Time_SSM_UTC	Universal Time (seconds since midnight)	seconds
6	GNSS_Easting_WGS84UTM55	WGS84UTM55 easting of the GNSS antenna observation	metres
7	GNSS_Northing_WGS84UTM55	WGS84UTM55 northing of the GNSS antenna observation	metres
8	GNSS_Longitude_WGS84	Observed WGS84 longitude of the GNSS antenna	degrees
9	GNSS_Latitude_WGS84	Observed WGS84 latitude of the GNSS antenna	degrees
10	Elevation_GNSS_GRS80	Observed GRS80 ellipsoid elevation of the GNSS antenna	metres
11	Elevation_GNSS_MSL	Observed EGM96 geoid elevation of the GNSS antenna (after application of undulation correction to GRS80 elevation data)	metres
12	Ground_Clearance_GGI_TCGrid_DSM_MSL	Clearance of the GGI above the Digital Surface Model (TCGrid_DSM_MSL) derived from the GGI elevation (MSL)	metres
13	TCGrid_DSM_MSL	Sampled from the Digital Surface Model (DSM) that was used for gravity terrain corrections	metres
14	Flux_x	Lagged Fluxgate component x	nanoteslas
15	Flux_y	Lagged Fluxgate component y	nanoteslas
16	Flux_z	Lagged Fluxgate component z	nanoteslas
17	Diurnal	Magnetic Ground Base Station	nanoteslas
18	IGRF	International Geomagnetic Reference Field based on date location and altitude of each point	nanoteslas
19	Mag_raw	Lagged Total Magnetic Intensity (Uncompensated)	nanoteslas
20	Mag_comp	Lagged Total Magnetic Intensity (Compensated)	nanoteslas
21	Mag_IGRF	Lagged Total Magnetic Intensity (Lagged Total Magnetic Intensity after Diurnal and IGRF correction)	nanoteslas
22	Mag_TMI	Lagged Total Magnetic Intensity (Levelled)	nanoteslas

Table 5: Final Aeromagnetic Digital Data – Geosoft Database Format

File	Description	Units
803064_TMI_Final	Total Magnetic Intensity	nT
803064_ TCGrid_DSM_MSL _Final	Digital terrain model (derived from laser scanner and 1 arc second SRTM data)	metres
803064_Drapesurface_Equiv_Final	Equivalent source drape surface	metres
803064_gD_Equiv_0_Conformed_Final	Equivalent source derived vertical gravity, conformed to regional gravity (no terrain correction applied)	mGal
803064_gD_Equiv_0_Final	Equivalent source derived vertical gravity (no terrain correction applied)	mGal
803064_gD_Equiv_2p67_Conformed_Final	Equivalent source derived vertical gravity, terrain correction density 2.67 g/cm^3 conformed to regional gravity	mGal
803064_gD_Equiv_2p67_Final	Equivalent source derived vertical gravity, terrain correction density 2.67 g/cm^3	mGal
803064_GDD_Equiv_0_Final	Equivalent source derived vertical gravity gradient (no terrain correction applied)	eotvos
803064_GDD_Equiv_2p67_Final	Equivalent source derived vertical gravity gradient, terrain correction density 2.67 g/cm^3	eotvos
803064_GED_Equiv_0_Final	Equivalent source derived GED horizontal EW gradient (no terrain correction applied)	eotvos
803064_GED_Equiv_2p67_Final	Equivalent source derived GED horizontal EW gradient (2.67 g/cm^3 terrain correction density)	eotvos
803064_GEE_Equiv_0_Final	Equivalent source derived GEE gradient (no terrain correction applied)	eotvos
803064_GEE_Equiv_2p67_Final	Equivalent source derived GEE gradient (2.67 g/cm^3 terrain correction density)	eotvos
803064_GND_Equiv_0_Final	Equivalent source derived GND horizontal NS gradient (no terrain correction applied)	eotvos
803064_GND_Equiv_2p67_Final	Equivalent source derived GND horizontal NS gradient (2.67 g/cm^3 terrain correction density)	eotvos
803064_GNE_Equiv_0_Final	Equivalent source derived GNE curvature gradient (no terrain correction applied)	eotvos
803064_GNE_Equiv_2p67_Final	Equivalent source derived GNE curvature gradient (2.67 g/cm^3 terrain correction density)	eotvos
803064_GNN_Equiv_0_Final	Equivalent source derived GNN gradient (no terrain correction applied)	eotvos
803064_GNN_Equiv_2p67_Final	Equivalent source derived GNN gradient (2.67 g/cm^3 terrain correction density)	eotvos
803064_GUV_Equiv_0_Final	Equivalent source derived GUV curvature gradient (no terrain correction applied)	eotvos
803064_GUV_Equiv_2p67_Final	Equivalent source derived GUV curvature gradient (2.67 g/cm^3 terrain correction density)	eotvos

Table 6: Final magnetic and AGG Grids – ERMapper Format